Combining cyanometalates and coordination clusters: an alternative synthetic route toward original molecular materials

ARTICLE *in* CRYSTAL GROWTH & DESIGN · AUGUST 2013

Impact Factor: 4.89

1 AUTHOR:

Abhishake Mondal

French National Centre for Scientific Research

18 PUBLICATIONS **90** CITATIONS

SEE PROFILE

CRYSTAL GROWTH & DESIGN

Communication

pubs.acs.org/crystal

Combining Cyanometalates and Coordination Clusters: An Alternative Synthetic Route toward Original Molecular Materials

Abhishake Mondal,[§] Pierre-Igor Dassié,[§] Lise-Marie Chamoreau,[§,⊥] Yves Journaux,[§,#] Miguel Julve,[‡] Laurent Lisnard,*[,§,#] and Rodrigue Lescouëzec*[,§]

[§]Institut Parisien de Chimie Moléculaire, UMR 7201, UPMC Univ. Paris 06, Paris, 75005, France

[#]Institut Parisien de Chimie Moléculaire, CNRS, UMR 7201, Paris, 75005, France

[⊥]Centre de résolution structurale, Institut Parisien de Chimie Moléculaire, Paris, 75005, France

[‡]Instituto de Ciencia Molecular (ICMol), Facultat de Química, Universitat de València, C/Catedrático José Beltrán 2, 46980 Paterna, València, Spain

Supporting Information

ABSTRACT: As an original synthetic route to molecular magnetic materials, we have reacted partially-blocked cyanometalates with preformed coordination cluster. The association of the *fac*-$[Fe(Tp)(CN)_3]^-$ assembling metalloligand with the $[Cu_3(OH)(pz)_3]^{2+}$ trigonal cluster has afforded a novel coordination network where the trimetallic copper(II) nodes are linked by the iron(III) complexes into chains and by coordinating acetate into a two-dimensional framework.

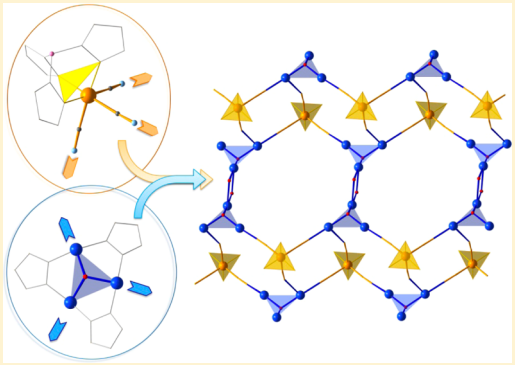

With the discovery of molecules or molecule-based compounds that can display blocked magnetization, magnetic ordering or switchable magnetic bistability, the research efforts devoted to molecular magnetic materials have increased considerably over the past two decades, fully exploiting the advantages of the bottom-up approach.[1−4] This research field focuses on promising properties for potential technological applications, such as information storage, quantum computing, and spintronics at the molecular scale, but it also provides fundamental insights into original quantum phenomena.[5,6] Coordination chemists have developed efficient synthetic tools for the preparation of interesting magnetic systems. Overall, two strategies are mainly used: the programmed assembly and the serendipitous self-assembly.[7] The former consists in the preparation of specific building blocks that possess desired topology and electronic information and their use to form predictable architectures with targeted magnetic properties. The latter lies on the use of sensibly chosen ligands that display multibinding modes and can thus promote magnetic exchange between several metal ions, with no assumptions or control on the shapes and the nuclearities of the final products. The programmed assembly approach is well-illustrated with the use of metalloligands containing oxalate, oxamate or Schiff-base ligands.[8−10] Cyanometalates also constitute excellent examples of tunable building blocks and they have successfully led to a broad variety of molecule-based magnets.[11,12] In particular, partially blocked cyanometalates have afforded single-chain magnets (SCMs), and they are especially relevant for the preparation of photomagnetic molecules.[13,14] With regard to the serendipitous self-assembly strategy, its efficiency is plainly demonstrated for the preparation of single-molecule magnets (SMMs), since serendipitously formed coordination clusters have provided to date the best examples of SMMs.[15,16] They furthermore represent a formidable class of polymetallic molecular compounds with an impressive variety of shapes, sizes, or compositions, and they can, in turn, be considered as attractive starting materials. Beside these two well-known synthetic approaches, the magneto-chemists are actively exploring new routes, aiming at the synthesis of sophisticated magnetic materials. For instance, the relatively recent use of polymetallic SMMs as building units and their further assembling through organic linkers has been established as an original strategy;[17,18] so has the use of paramagnetic cyanometalates to connect compartmental-ligand-based heterometallic complexes.[19−23] The latter approach has indeed been established as a reliable route toward heterotrimetallic paramagnetic complexes.[23] Nonetheless, the former strategy focuses primarily on SMMs as building blocks, and it remains not yet fully investigated with paramagnetic linkers, and the latter one lies so far on

Received: July 24, 2013
Revised: August 27, 2013

   dx.doi.org/10.1021/cg401117u | *Cryst. Growth Des.* XXXX, XXX, XXX−XXX

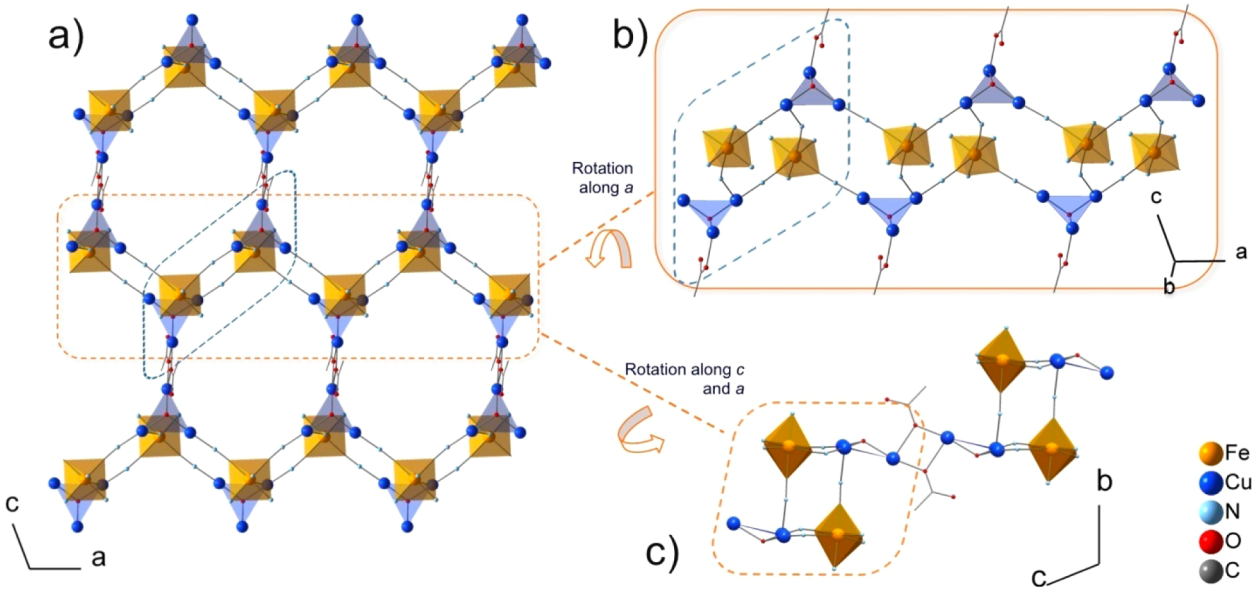

Figure 1. Schematic view of the 2D structuring of **1** in the crystal. Tp and pz ligands and solvent molecules as well as the hydrogen atoms have been omitted for clarity.

polymetallic building blocks that could seem, when compared to oxo/carboxylato coordination clusters, limited in terms of nuclearity or lacking flexibility. Alternatively, we have undertaken the study of the reactivity of cyanide-bearing metalloligands toward carboxylato-based clusters, our first result consisting of a unique cubic nanocage where the apexes are defined by *fac*-[Fe(Tp)(CN)$_3$] units and {Co$_3$(μ_3−OH)(piv)$_4$} triangles [Tp = tris(pyrazolyl)borate, Hpiv = 2,2′-dimethylpropionic acid, commonly referred as pivalic acid)].[24] This appealing preliminary result led us to investigate the reactivity of the *fac*-[Fe(Tp)(CN)$_3$]$^-$ complex toward other trigonal hydroxo-bridged coordination clusters. We present here the preparation, crystal structure determination, and preliminary magnetic study of the novel two-dimensional (2D) compound of formula [{Fe(Tp)(μ-CN)$_3$}$_2${Cu$_3$(μ_3−OH)(μ-pz)$_3$(μ-OOCCH$_3$)(H$_2$O)$_{0.5}$}$_2$]·EtOH (**1**) (pz = pyrazolate), which results from the assembling of the mononuclear complex [Fe(Tp)(CN)$_3$]$^-$ and the hydroxo-centered tricopper(II) unit [Cu$_3$(μ_3−OH)(μ-pz)$_3$]$^{2+}$ (see the Supporting Information for experimental details).

1 crystallizes in the $P\bar{1}$ space group[25] with a neutral heterobimetallic 2D structure extending the *ac* plane (Figure 1a). Each layer is constituted by zigzag ladderlike chains running parallel to the crystallographic *a* axis where regular alternating tris-monodentate [Fe(1)(Tp)(CN)$_3$]$^-$ units and the Cu(1)/Cu(2) atoms from the [Cu$_3$(μ_3−OH)(μ-pz)$_3$(OOCCH$_3$)]$^+$ triangles occur along the rods, the rungs being defined by centrosymmetric Fe(1)Cu(1)Fe(1a)Cu(1a) square motifs [symmetry code: (a) = −1 − *x*, 2 − *y*, 1 − *z*] (Figure 1b). These double chains are further interlinked along the crystallographic *c* axis by double μ-oxo(acetate) bridges involving the outer Cu(3) and Cu(3c) atoms [symmetry code: (c) = 2 − *x*, 2 − *y*, 2 − *z*] from tricopper(II) units of adjacent chains (Figure 1c). The resulting layers exhibit a parallel stacking along the *b* axis, and they are well-separated from each other, the shortest interlayer metal−metal distance being 8.7657(9) Å (Figure S1 of the Supporting Information).

Each iron(III) ion is coordinated by three Tp-nitrogen atoms and three cyanide-carbon atoms with a C_{3v} symmetry

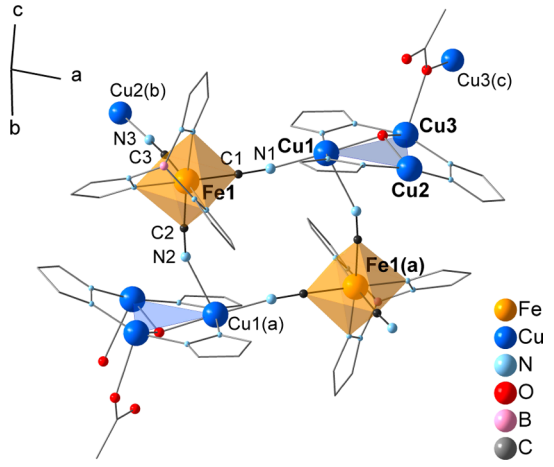

Figure 2. Representation of the {Fe$_2$(Cu$_3$)$_2$} square building unit in **1**. The hydrogen atoms are omitted for clarity. [Symmetry codes: (a) = −1 − x, 2 − y, 1 − z; (b) = −1 + x, y, z; (c) = 2 − x, 2 − y, 2 − z].

(Figure 2). The values of the three Fe(1)-C distances are in the very narrow 1.909(4)−1.922(4) Å range, and they are in agreement with those observed in previous magneto-structurally characterized low-spin iron(III) mononuclear species containing the *fac*-[Fe(Tp)(CN)$_3$]$^-$ anion [1.910(6)-1.930(3) Å].[26,27] The cyanide stretching vibration [ν(C≡N)] in the infrared spectrum of **1** is located at 2162 cm^{-1} (see the Supporting Information), and it is consistent with the presence of bridging cyanide only (to be compared with peaks in the 2118−2129 cm^{-1} range for the terminal cyanide ligands in the mononuclear *fac*-[Fe(Tp)(CN)$_3$]$^-$ species). The Fe(1)−C≡N angles are close to linearity with values ranging from 172.6(3) to 175.8(4)°. However, a significant bending is observed on the edges of the Fe(1)Cu(1)Fe(1a)Cu(1a) square motifs [Cu(1)−N(1)−C(1) = 164.9(3)° and Cu(1)−N(2)−C(2) = 150.7(4)°] (Figure 2), whereas the intersquare Fe(1)−C−N−Cu(2b) bridge is closer to linearity [Cu(2b)−N(3)−C(3) = 176.0(3)°; symmetry code: (b) = −1 + *x*, *y*, *z*]. The iron−copper distances across the cyanide bridges in **1** are 5.00543(8), 4.9834(6), and

dx.doi.org/10.1021/cg401117u | *Cryst. Growth Des.* XXXX, XXX, XXX−XXX

5.1316(8) Å for Fe(1)···Cu(2b), Fe(1)···Cu(1), and Fe(1)···Cu(1a), respectively, and compare well with those previously reported for discrete rectangular[28] and pentanuclear motifs,[29] as well as in 1D compounds that display a similar fragment.[30−32]

As in the parent compound of formula $[Cu_3(\mu-OH)(\mu-pz)_3(Hpz)(NO_3)_2]$,[33] the tricopper(II) unit in **1** can be described as a triangle with the Cu(1), Cu(2), and Cu(3) atoms at the apexes, single pyrazolate ligands along the edges, and a μ_3-hydroxo group capping the triangle (the oxygen atom is located at 0.6 Å from the triangle plane). The copper−copper distances within the triangle are in the 3.2262(7)−3.3847(7) Å range [av. 3.30 Å]. In the pyramidal $\{Cu_3(\mu-OH)\}$ core, the three Cu−O(1) bond distances range from 1.986(2) to 2.026(2), and the values of the Cu−O(1)−Cu' angles are found between 106.84(12) and 116.65(12)°. In the peripheral $\{Cu(N-N)\}_3$ ring, the Cu−N distances are homogeneous, from 1.942(3) to 1.952(3) Å. Cu(1) and Cu(3) are five-coordinate with two pyrazolate-nitrogen, the hydroxo-oxygen and either two cyanide-nitrogen [Cu(1)] or two carboxylate-oxygen atoms [Cu(3)] building distorted square pyramidal surroundings. Cu(2) is alternatively in square pyramidal [Cu(2)N(15)N(10)O(1)N(3)O(4)] or in square planar [Cu(2)(N15)N(10)O(1)N(3)] environments, depending on the presence or absence of a coordinated water molecule [O(4)]. The [Cu(3)O(2)O(2c)Cu(3c)] fragment that results from the double μ-acetato bridge linking the chains has copper(II) ions coordinated to oxygen atoms in equatorial and axial positions, the Cu−O bond lengths being 1.981(3) and 2.348(3) Å, respectively, and the bridgehead angle [Cu(3)−O(2)−Cu(3c)] being 102.4(1)°. Hydrogen bonds involving the coordinated water molecule, the hydroxo group, and the uncoordinated acetate oxygen atom [O(1)···O(3) = 2.791(5)Å and O(3)···O(4) = 2.62(1)Å] contribute to the stabilization of the layered structure (Figure S2 of the Supporting Information).

In our previous work,[24] the *fac*-$[Fe(Tp)(CN)_3]^-$ unit acted as a tris-monodentate ligand toward three cobalt(II) ions from three different $\{Co_3\}$ triangles. In each triangle, the cobalt atoms were thus coordinated to three different iron atoms through orthogonal cyanide ligands, leading to a discrete cubic motif. The rigidity of the metalloligand undoubtedly played an important role in the formation of this geometry. In the present study, we have used a trigonal $\{Cu_3\}$ building block exhibiting a similar shape to that of the $\{Co_3\}$ triangles. As in the case of the cobalt triangles, the *fac*-$[Fe(Tp)(CN)_3]^-$ unit adopts a tris-monodentate coordination mode toward three copper(II) ions from three $\{Cu_3\}$ triangles. Although the orthogonal arrangement of the cyanide ligands favors the $[Fe_2Cu_2]$ square motifs, the presence of a competitive bridging ligand, the acetate ion, is responsible for the formation of the unprecedented 2D architecture in **1**.

Variable-temperature dc magnetic susceptibility measurements have been performed on a crushed polycrystalline sample of **1** under applied dc magnetic fields of 2.5 kOe (2−300 K) and 250 Oe (2−30 K). The $\chi_M T$ versus T plot (where χ_M is the molar magnetic susceptibility per $\{Fe^{III}_2Cu^{II}_6\}$ unit) is shown in Figure 3. The $\chi_M T$ value at room temperature is 2.19 $cm^3\ mol^{-1}$ K, a value that is well below the calculated one for a set of two low-spin iron(III) and six copper(II) ions magnetically noninteracting ($\chi_M T$ = 3.75 $cm^3\ mol^{-1}$ K with $S_{Fe} = S_{Cu} = 1/2$, $g_{Fe} = 2.6$, and $g_{Cu} = 2.1$).[34] Upon cooling, $\chi_M T$ smoothly decreases to attain a quasi plateau between 80 and 40 K (with $\chi_M T \sim 1.7$ cm^3 K mol^{-1}) and it further sharply

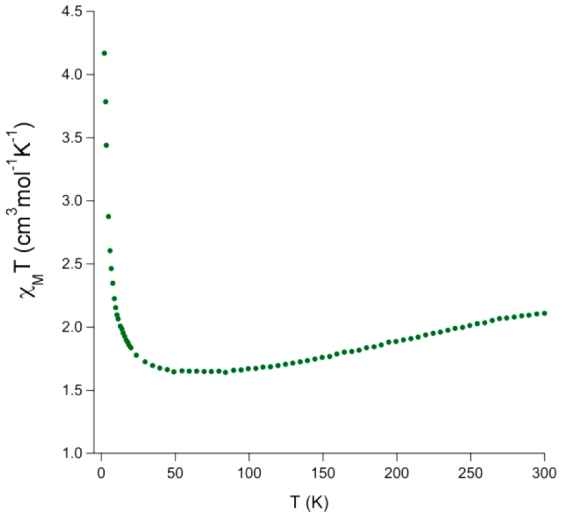

Figure 3. $\chi_M T$ vs T plot for **1**, measured at 2.5 kOe between 300 and 2.0 K.

increases to 4.33 $cm^3\ mol^{-1}$ K at 2.0 K. The interpretation and analysis of these magnetic data are made difficult by the complex topology of **1** and the coexistence of various exchange pathways: (i) the cyanide bridges between the low-spin iron(III) and the copper(II) ions within the ladderlike motif, (ii) the hydroxo and pyrazolate bridges in the tricopper(II) units, (iii) and the double oxo(acetate) connection between copper(II) ions from adjacent ladderlike chains.

There is no model to treat the magnetic data of **1**, but a qualitative description of its magnetic behavior can be made in the light of the results found in the literature concerning the three exchange pathways involved here. First of all, the small $\chi_M T$ value observed at room temperature points out the occurrence of significant antiferromagnetic exchange interactions. Indeed, the pyrazolate hydroxo-centered $\{Cu_3\}$ clusters are known to exhibit both strong antiferromagnetic couplings ($150 < |J| < 210$ cm^{-1}) and significant antisymmetric exchange interactions, resulting in 1/2 ground spin states.[35] In contrast, the other two exchange pathways exhibit weak exchange interactions. The orbital contribution of the low-spin iron(III) centers and the relatively strong antiferromagnetic interaction in the tricopper(II) triangles should thus be responsible for the observed decrease of $\chi_M T$ in the high-temperature region. A smaller ferromagnetic coupling between the low-spin iron(III) and the resulting spin doublet from the tricopper(II) unit would account for the increase of the $\chi_M T$ value in the low-temperature domain. Indeed, ferromagnetic interactions varying from +17 to +34.4 cm^{-1} have been reported for magneto-structurally characterized examples of $\{Fe^{III}(Tp)(CN)_2(\mu-CN)Cu^{II}\}$ motifs.[28−32] The possible magnetic coupling through the double oxo(acetate) bridge is necessarily weak. It corresponds to an equatorial−axial exchange pathway and the literature data reveal that its ability to mediate magnetic interactions is very low (J values from −2.36 to +1.95 cm^{-1}).[36] The shape of the M vs H plot at 2.0 K (Figure S3 of the Supporting Information) supports the occurrence of a ferromagnetic interaction between the low-spin iron(III) and the doublet-spin state of the tricopper(II) unit within the ladderlike motif. In addition, the absence of inflection point in such a curve at very low applied fields is consistent with an extremely weak interchain antiferromagnetic interaction (if any) through the (iii) pathway or with a very weak

dx.doi.org/10.1021/cg401117u | *Cryst. Growth Des.* XXXX, XXX, XXX−XXX

ferromagnetic coupling across it. Most likely, the magnetic behavior observed for **1** obeys the (i) and (ii) pathways.

The $\{Cu_3(\mu_3\text{–}OH)(\mu\text{-pz})_3\}$ cluster has been successfully used to generate supramolecular assemblies and multidimensional networks when associated with organic linkers or coordinating counter-anions, such as acetate.[33,37−43] Here, we extend its use with the first example of its assembling with a metalloligand. Similarly, the *fac*-$[Fe(Tp)(CN)_3]^-$ complex used as a metalloligand is known to yield molecular or one-dimensional assemblies with paramagnetic ions,[44] **1** being the first example of a $\{Fe(Tp)(CN)_3\}$-based 2D network. Of course, the nature of the trimetallic node and the role of the acetate ligand are far from innocent in this assembly process. More generally, the originality of **1** highlights the benefits one can gain associating cyanometalates with coordination clusters. Indeed, the impressive amount of accessible coordination clusters provides a fascinating set of building blocks with many tunable parameters (nuclearity, charge, geometry, flexibility, coligand, etc.). Their association with the comparably rich family of tunable cyanometalate building blocks constitutes therefore a formidable study where uncommon architectures should undoubtedly be encountered and where the relationship between the starting materials' intrinsic features and the assembled entities' properties, once explored, should lead to interesting magnetic properties.

■ ASSOCIATED CONTENT

Supporting Information

X-ray crystallographic files for **1** in cif format; experimental details for the preparation and the characterization of **1**; figures detailing crystal packing (Figure S1); the hydrogen bonds (Figure S2); plots of M vs H (Figure S3), χ_M vs T, and $1/\chi_M$ vs T (Figure S4) for **1**. This material is available free of charge via the Internet at http://pubs.acs.org.

■ AUTHOR INFORMATION

Corresponding Author

*R.L.: e-mail, rodrigue.lescouezec@upmc.fr. L.L.: e-mail, laurent.lisnard@upmc.fr; tel, +33 1 44 27 30 75; fax, +33 1 44 27 38 41.

Notes

The authors declare no competing financial interest.

■ ACKNOWLEDGMENTS

This work was supported by the Ministère de l'Enseignement Supérieur et de la Recherche (MESR, France), the Centre National de la Recherche Scientifique (CNRS), the Erasmus Mundus program (lot 13), the Agence Nationale de la Recherche (Project ANR-08-BLAN-0186-01), the Ministerio Español de Ciencia e Innovación (Project CTQ 2010-15364), and the Generalitat Valenciana (ISIC2012/002). We acknowledge SOLEIL for the provision of synchrotron radiation facilities, and we would like to thank Pierre Fertey for his help and support in using the CRISTAL beamline (Proposal 20120026).

■ REFERENCES

(1) *Book series, "Magnetism: Molecules to Materials" I–V*; Miller, J. S., Drillon, M., Eds.; Wiley-VCH: Weinheim, 2005.

(2) Special issue on Molecular Magnets *Dalton Trans.* **2010**, *39*, 4653−5040.

(3) Special issue on Molecular Magnets *Chem. Soc. Rev.* **2011**, *40*, 3053−3368.

(4) Special issue: Frontier and Perspectives in Molecule-Based Quantum Magnet *Dalton Trans.* **2012**, *41*, 13543−13766.

(5) Gatteschi, D.; Sessoli, R.; Villain, J. *Molecular Nanomagnets (Mesoscopic Physics and Nanotechnology)*; OUP: Oxford, 2006.

(6) Winpenny, R. E. P.; McInnes, E. J. L. In *Molecular Materials*; John Wiley & Sons, Ltd: Hoboken, NJ, 2010; pp 281−348.

(7) Winpenny, R. E. P. *J. Chem. Soc., Dalton Trans.* **2002**, 1−10.

(8) Dul, M.-C.; Pardo, E.; Lescouëzec, R.; Journaux, Y.; Ferrando-Soria, J.; Ruiz-Garcia, R.; Cano, J.; Julve, M.; Lloret, F.; Cangussu, D.; Pereira, C. L. M.; Stumpf, H. O.; Pasan, J.; Ruiz-Perez, C. *Coord. Chem. Rev.* **2010**, *254*, 2281−2296.

(9) Marinescu, G.; Andruh, M.; Lloret, F.; Julve, M. *Coord. Chem. Rev.* **2011**, *255*, 161−185.

(10) Andruh, M.; Costes, J.-P.; Diaz, C.; Gao, S. *Inorg. Chem.* **2009**, *48*, 3342−3359.

(11) Shatruk, M.; Avendano, C.; Dunbar, K. R. *Prog. Inorg. Chem.* **2009**, *56*, 155−334.

(12) Rebilly, J.-N.; Mallah, T. *Struct. Bonding (Berlin, Ger.)* **2006**, *122*, 103−131.

(13) Lescouëzec, R.; Toma, L. M.; Vaissermann, J.; Verdaguer, M.; Delgado, F. S.; Ruiz-Perez, C.; Lloret, F.; Julve, M. *Coord. Chem. Rev.* **2005**, *249*, 2691−2729.

(14) Newton, G. N.; Nihei, M.; Oshio, H. *Eur. J. Inorg. Chem.* **2011**, *2011*, 3031−3042.

(15) Milios, C. J.; Vinslava, A.; Wernsdorfer, W.; Moggach, S.; Parsons, S.; Perlepes, S. P.; Christou, G.; Brechin, E. K. *J. Am. Chem. Soc.* **2007**, *129*, 2754−2755.

(16) Blagg, R. J.; Muryn, C. A.; McInnes, E. J. L.; Tuna, F.; Winpenny, R. E. P. *Angew. Chem., Int. Ed.* **2011**, *50*, 6530−3.

(17) Miyasaka, H.; Yamashita, M. *Dalton Trans.* **2007**, 399.

(18) Roubeau, O.; Clérac, R. *Eur. J. Inorg. Chem.* **2008**, 4325−4342.

(19) Andruh, M. *Chem. Commun.* **2011**, *47*, 3025−3042.

(20) Jeon, I.-R.; Clérac, R. *Dalton Trans.* **2012**, *41*, 9569.

(21) Long, J.; Chamoreau, L.-M.; Mathonière, C.; Marvaud, V. *Inorg. Chem.* **2009**, *48*, 22−24.

(22) Alexandru, M.-G.; Visinescu, D.; Madalan, A. M.; Lloret, F.; Julve, M.; Andruh, M. *Inorg. Chem.* **2012**, *51*, 4906−4908.

(23) Palacios, M. A.; Mota, A. J.; Ruiz, J.; Hänninen, M. M.; Sillanpää, R.; Colacio, E. *Inorg. Chem.* **2012**, *51*, 7010−7012.

(24) Mondal, A.; Durdevic, S.; Chamoreau, L.-M.; Journaux, Y.; Julve, M.; Lisnard, L.; Lescouëzec, R. *Chem. Commun.* **2013**, *49*, 1181−1183.

(25) XRD measurements have been performed in the Soleil synchrotron in Gif-sur-Yvette, France, on the CRISTAL beamline; see Supporting Information for details.

(26) Lescouëzec, R.; Vaissermann, J.; Lloret, F.; Julve, M.; Verdaguer, M. *Inorg. Chem.* **2002**, *41*, 5943−5945.

(27) Kim, J.; Han, S.; Cho, I.-K.; Choi, K. Y.; Heu, M.; Yoon, S.; Suh, B. J. *Polyhedron* **2004**, *23*, 1333−1339.

(28) Liu, W.; Wang, C.-F.; Li, Y.-Z.; Zuo, J.-L.; You, X.-Z. *Inorg. Chem.* **2006**, *45*, 10058−10065.

(29) Wang, C.-F.; Zuo, J.-L.; Bartlett, B. M.; Song, Y.; Long, J. R.; You, X.-Z. *J. Am. Chem. Soc.* **2006**, *128*, 7162−7163.

(30) Wang, S.; Zuo, J.-L.; Gao, S.; Song, Y.; Zhou, H.-C.; Zhang, Y.-Z.; You, X.-Z. *J. Am. Chem. Soc.* **2004**, *126*, 8900−8901.

(31) Wang, S.; Zuo, J.-L.; Zhou, H.-C.; Song, Y.; Gao, S.; You, X.-Z. *Eur. J. Inorg. Chem.* **2004**, *2004*, 3681−3687.

(32) Wen, H.-R.; Wang, C.-F.; Song, Y.; Gao, S.; Zuo, J.-L.; You, X.-Z. *Inorg. Chem.* **2006**, *45*, 8942−8949.

(33) Hulsbergen, F. B.; Ten, H.; Verschoor, G. C.; Reedijk, J.; Spek, A. L. *J. Chem. Soc., Dalton Trans.* **1983**, 539−45.

(34) Figgis, B. N.; Lewis, J.; Mabbs, F. E.; Webb, G. A. *J. Chem. Soc. A* **1967**, 442−447.

(35) Ferrer, S.; Lloret, F.; Pardo, E.; Clemente-Juan, J. M.; Liu-González, M.; García-Granda, S. *Inorg. Chem.* **2012**, *51*, 985−1001.

(36) Simões, T. R. G.; Mambrini, R. V.; Reis, D. O.; Marinho, M. V.; Ribeiro, M. A.; Pinheiro, C. B.; Ferrando-Soria, J.; Déniz, M.; Ruiz-Pérez, C.; Cangussu, D.; Stumpf, H. O.; Lloret, F.; Julve, M. *Dalton Trans.* **2013**, *42*, 5778−5795 and references therein.

(37) Casarin, M.; Corvaja, C.; Nicola, C.; di Falcomer, D.; Franco, L.; Monari, M.; Pandolfo, L.; Pettinari, C.; Piccinelli, F.; Tagliatesta, P. *Inorg. Chem.* **2004**, *43*, 5865−5876.
(38) Casarin, M.; Corvaja, C.; Di, N.; Falcomer, D.; Franco, L.; Monari, M.; Pandolfo, L.; Pettinari, C.; Piccinelli, F. *Inorg. Chem.* **2005**, *44*, 6265−6276.
(39) Casarin, M.; Cingolani, A.; Di, N.; Falcomer, D.; Monari, M.; Pandolfo, L.; Pettinari, C. *Cryst. Growth Des.* **2007**, *7*, 676−685.
(40) Contaldi, S.; Di, N.; Garau, F.; Karabach, Y. Y.; Martins, L. M. D. R. S.; Monari, M.; Pandolfo, L.; Pettinari, C.; Pombeiro, A. J. L. *Dalton Trans.* **2009**, 4928−4941.
(41) Di Nicola, C.; Garau, F.; Gazzano, M.; Monari, M.; Pandolfo, L.; Pettinari, C.; Pettinari, R. *Cryst. Growth Des.* **2010**, *10*, 3120−3131.
(42) Rivera-Carrillo, M.; Chakraborty, I.; Raptis, R. G. *Cryst. Growth Des.* **2010**, *10*, 2606−2612.
(43) Di Nicola, C.; Garau, F.; Gazzano, M.; Guedes, da S.; Lanza, A.; Monari, M.; Nestola, F.; Pandolfo, L.; Pettinari, C.; Pombeiro, A. J. L. *Cryst. Growth Des.* **2012**, *12*, 2890−2901.
(44) Wang, S.; Ding, X.-H.; Zuo, J.-L.; You, X.-Z.; Huang, W. *Coord. Chem. Rev.* **2011**, *255*, 1713−1732.

dx.doi.org/10.1021/cg401117u | *Cryst. Growth Des.* XXXX, XXX, XXX−XXX